

AFWAL-TR-87-4020

ADA 181069



MORPHOLOGY OF A PHASE SEPARATED AND A MOLECULAR
COMPOSITE 30% PBT/70% ABPBI BLOCK COPOLYMER

W. W. Adams
Polymer Branch
Nonmetallic Materials Division

S.J. Krause and T. B. Haddock
Dept. of Mechanical and Aerospace Engineering
Arizona State University
Tempe, AZ 85287

G. E. Price
University of Dayton Research Institute
Dayton, OH 45469

January 1987

Interim Report for Period January to December 1985

Approved for Public Release; Distribution Unlimited

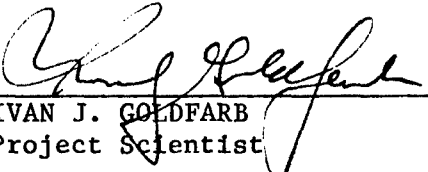
MATERIALS LABORATORY
AIR FORCE WRIGHT AERONAUTICAL LABORATORIES
AIR FORCE SYSTEMS COMMAND
WRIGHT-PATTERSON AFB, OH 45433-6533

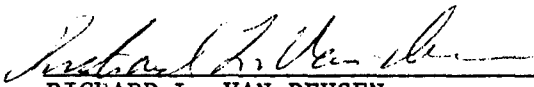
200 402 19 207

When Government drawings, specifications, or other data are used for any purpose other than in connection with a definitely related Government procurement operation, the United States Government thereby incurs no responsibility nor any obligation whatsoever; and the fact that the Government may have formulated, furnished, or in any way supplied the said drawings, specifications, or other data, is not to be regarded by implication or otherwise as in any manner licensing the holder or any other person or corporation, or conveying any rights or permission to manufacture use, or sell any patented invention that may in any way be related thereto.


This report has been reviewed by the Office of Public Affairs (ASD/PA) and is releasable to the National Technical Information Service (NTIS). At NTIS, it will be available to the general public, including foreign nationals.

This technical report has been reviewed and is approved for publication.


IVAN J. GOLDFARB
Project Scientist


RICHARD L. VAN DEUSEN
Chief, Polymer Branch

FOR THE COMMANDER


MERRILL L. MINGES, PhD, SES
Director
Nonmetallic Materials Division

"If your address has changed, if you wish to be removed from our mailing list, or if the addressee is no longer employed by your organization please notify AFWAL/MLBP, Wright-Patterson AFB OH 45433 to help us maintain a current mailing list."

Copies of this report should not be returned unless return is required by security considerations, contractual obligations, or notice on a specific document.

Unclassified

SECURITY CLASSIFICATION OF THIS PAGE

REPORT DOCUMENTATION PAGE

1a. REPORT SECURITY CLASSIFICATION Unclassified			1b. RESTRICTIVE MARKINGS	
2a. SECURITY CLASSIFICATION AUTHORITY			3. DISTRIBUTION/AVAILABILITY OF REPORT Approved for Public Release, distribution unlimited.	
2b. DECLASSIFICATION/DOWNGRADING SCHEDULE			5. MONITORING ORGANIZATION REPORT NUMBER(S)	
4. PERFORMING ORGANIZATION REPORT NUMBER(S) AFWAL-TR-87-4020				
6a. NAME OF PERFORMING ORGANIZATION Materials Laboratory		6b. OFFICE SYMBOL (If applicable) AFWAL/MLBP	7a. NAME OF MONITORING ORGANIZATION	
6c. ADDRESS (City, State and ZIP Code) Wright-Patterson AFB, OH 45433-6533			7b. ADDRESS (City, State and ZIP Code)	
8a. NAME OF FUNDING/SPONSORING ORGANIZATION		8b. OFFICE SYMBOL (If applicable)	9. PROCUREMENT INSTRUMENT IDENTIFICATION NUMBER	
8c. ADDRESS (City, State and ZIP Code)			10. SOURCE OF FUNDING NOS.	
			PROGRAM ELEMENT NO.	PROJECT NO.
			61102F	2303
			TASK NO.	WORK UNIT NO.
			Q3	07
11. TITLE (Include Security Classification) Morphology of a Phase Separated & a Molecular				
12. PERSONAL AUTHOR(S) W.W. Adams; S. J. Krause*, T. B. Haddock;* G. E. Price**				
13a. TYPE OF REPORT Interim		13b. TIME COVERED FROM Jan 85 TO Dec 85		14. DATE OF REPORT (Yr., Mo., Day) January 1987
15. PAGE COUNT 49				
16. SUPPLEMENTARY NOTATION *Arizona State University **University of Dayton Research Institute				
17. COSATI CODES			18. SUBJECT TERMS (Continue on reverse if necessary and identify by block number)	
FIELD	GROUP	SUB. GR.		
07	04		Block copolymer ABPBI Morphology	
11	04		PBT Rigid rod polymers Molecular composite	
19. ABSTRACT (Continue on reverse if necessary and identify by block number)				
<p>The morphology of a triblock copolymer of rigid-rod poly(p-phenylene benzobisthiazole (PBT) and semi-flexible coil poly (2,5(6)benzimidazole) (ABPBI) was examined by wide angle x-ray scattering and scanning and transmission electron microscopy. When samples were vacuum cast from a solution where the amount of 30% PBT/70% ABPBI copolymer was greater than a critical concentration of 5.8%, large-scale phase separation occurred and a film formed containing 0.1-micron particles and platelets in a ductile matrix. The particles and platelets were composed of well-oriented 10-nm PBT crystallites, while the matrix material was chiefly composed of ABPBI. When the amount of 30%PBT/70% ABPBI copolymer in a solvent was less than the critical concentration, the solution was optically homogeneous. Fibers which were dry-jet/wet-spun from the homogeneous solution into a water coagulating bath had large scale phase separation inhibited. After heat treatment the fiber contained crystallites of PBT and ABPBI with lateral dimensions no larger than 3nm, demonstrating that PBT molecular secements were well-dispersed and that a rigid-rod molecular level composite had been</p>				
20. DISTRIBUTION/AVAILABILITY OF ABSTRACT UNCLASSIFIED/UNLIMITED <input type="checkbox"/> SAME AS RPT. <input checked="" type="checkbox"/> DTIC USERS [21. ABSTRACT SECURITY CLASSIFICATION Unclassified	
22a. NAME OF RESPONSIBLE INDIVIDUAL W. W. Adams			22b. TELEPHONE NUMBER (Include Area Code) 513-255-9148	22c. OFFICE SYMBOL AFWAL/MLBP

Unclassified

SECURITY CLASSIFICATION OF THIS PAGE

11. Composite 30%PBT/70% ABPBI Block Copolymer

19. achieved. In the "molecular composite" copolymer fiber both the molecular level dispersion and high orientation resulted in excellent mechanical properties with a modulus of 100 GPa and a tensile strength of 1.7 GPa. Compared to phase-separated copolymer film, the "molecular composite" fiber had a modulus 26 times larger and a tensile strength 8 times larger.

Unclassified

SECURITY CLASSIFICATION OF THIS PAGE

FOREWORD

This report was prepared by the Polymer Branch, Nonmetallic Materials Division, the University of Dayton Research Institute, and Arizona State University. The work was initiated under Project No. 2303, "Research to Define the Structure Property Relationships," Task No. 2303Q3 Work Unit Directive 2303Q307, "Structural Resins." Dr. Thaddeus E. Helminiak served as the AFWAL/ML Work Unit Scientist. Co-authors were Dr. W. Wade Adams, Materials Laboratory (AFWAL/MLBP); Gary E. Price, University of Dayton Research Institute; and Dr. Stephen J. Krause and Tim Haddock, Arizona State University. This report covers research conducted from January to December 1985.

TABLE OF CONTENTS

SECTION	PAGE
I. INTRODUCTION	1
II. BACKGROUND	3
1. PBT Fiber	3
2. ABPBI Fiber	4
3. Polymer Phase Compatibility	5
4. Physical Blend Cast Film	7
5. Physical Blend Spun Fiber	8
6. Copolymer Film and Fiber	9
III. EXPERIMENTAL METHODS	11
1. Materials Processing	11
2. Scanning Electron Microscopy	12
3. Wide Angle X-ray Diffraction	12
4. Transmission Electron Microscopy	12
IV. RESULTS AND DISCUSSION	13
1. Scanning Electron Microscopy	13
a. Copolymer Cast Film	13
b. Copolymer Spun Fiber	14
2. Wide Angle X-ray Diffraction	17
a. Copolymer Cast Film	17
b. Copolymer Spun Fiber	20

TABLE OF CONTENTS (Concluded)

SECTION	PAGE
3. Transmission Electron Microscopy Imaging and Diffraction	23
a. Copolymer Cast Film	23
b. Copolymer Spun Fiber	24
4. General discussion	25
V. SUMMARY AND CONCLUSIONS	29
REFERENCES	31

LIST OF ILLUSTRATIONS

FIGURE		PAGE
1	Chemical and Molecular Structure of a PBT/ABPBI Triblock Copolymer	33
2	Models for Morphology of a 30% PBT/70% ABPBI Physical Blend a) Vacuum Cast Film from $C > C_{cr}$ Solution and b) Spun Fiber from $C < C_{cr}$ Solution	34
3	SEM Images of 30% PBT/70% ABPBI Vacuum Cast Copolymer Film at a) Lower Magnification and b) at Higher Magnification	35
4	SEM Images of 30% PBT/70% ABPBI Spun Copolymer Fiber at a) Lower Magnification and b) at Higher Magnification	36
5	Models for morphology of a 30% PBT/70% ABPBI Copolymer a) Vacuum Cast Film from $C > C_{cr}$ Solution and b) Spun Fiber from $C < C_{cr}$ Solution	37
6	WAXS Laue Photographs of a) PBT Fiber, b) ABPBI Fiber, c) 30% PBT/70% ABPBI Physical Blend Vacuum Cast Film d) 30% PBT/70% ABPBI Physical Blend Spun Fiber e) 30% PBT/70% ABPBI Copolymer Vacuum Cast Film f) 30% PBT/70% ABPBI Copolymer Spun Fiber	38
7	TEM of 30% PBT/70% ABPBI Vacuum Cast Copolymer Film showing a) Dark Field Image, b) SAED Pattern from $5\mu\text{m}$ Area, and c) SAED Pattern from $0.1\mu\text{m}$ Area	39
8	TEM of 30% PBT/70% ABPBI Spun Copolymer Fiber showing a) Dark Field Image and b) SAED Pattern	40

LIST OF TABLES

TABLE		PAGE
1	Mechanical Testing Results for PBT, ABPBI, and 30% PBT/70% ABPBI Fiber and Film	10
2	The WAXS d-spacings for PBT, ABPBI, and 30% PBT/70% ABPBI Physical Blend Film and Fiber, and 30% PBT/70% ABPBI Copolymer Film and Fiber	19

SECTION I

INTRODUCTION

Currently, there is increasing interest in fabrication of rigid-rod molecular composites. A molecular composite is defined as a polymeric material consisting of two or more components which are dispersed at the molecular level at a scale no greater than a few nm. The purpose of forming a rigid-rod molecular composite is to reinforce a ductile matrix polymer with stiff, strong, rigid-rod polymer molecules. After synthesis, the key to producing a molecular composite is in controlling the morphology of the system in order to achieve the finest possible dispersion of the reinforcing rod molecules. Approaches to producing a molecular composite include special processing techniques and specific chemical synthesis methods. We report here the morphology of a new rigid-rod and flexible-coil triblock copolymer processed by different methods.

One method for producing a rigid-rod molecular composite is to create an intimate physical blend of rigid-rod molecules and flexible-coil molecules [1,2]. Takayanagi [3,4] studied several stiff-chain / flexible-coil polymer blends. He found that processing a blend of poly(p-phenylene terephthalamide) (PPTA) and nylon 6 or nylon 6/6 resulted in a dispersion of the reinforcing phase PPTA in the form of 30-nm-diameter microfibrils throughout the matrix material. Hwang *et al.* [5] processed blends of rigid-rod poly(p-phenylene benzobisthiazole) (PBT) and semi-flexible coil poly-2,5(6) benzimidazole (ABPBI) into fiber and film. It was found that large-scale phase separation was prevented when an optically homogeneous solution of 30% PBT/70% ABPBI was dry spun and then rapidly coagulated in water. In morphological studies of the 30% PBT/70% ABPBI heat-treated fiber and film by Krause and Adams [6] and Krause *et al.* [7], no phase

separation was observed at a scale greater than 3 nm when samples were examined by wide-angle x-ray scattering (WAXS) and scanning electron microscopy (SEM) and transmission electron microscopy (TEM). This demonstrated that a molecular composite had been achieved. A comparison of the moduli of oriented fiber of the PBT and ABPBI homopolymers to that of the physical blend also indicated that a molecular composite had been achieved according to the "rule of mixtures" for a uniaxially reinforced composite [5].

An alternative approach to physical blending of polymers for producing a molecular composite is to synthesize a block copolymer composed of flexible-coil segments and of rigid-rod block segments [8]. Takayanagi [3,4] studied a stiff-chain Aramid / flexible-coil nylon 6 copolymer and found that a "fine dispersion" of the components was achieved, although the size of the dispersed phase was not quantified. Tsai et al. [8] have recently reported on the synthesis and properties of a triblock copolymer of PBT and ABPBI. The chemical and molecular structure of the copolymer is shown in Figure 1: *A comparison of the moduli of oriented fiber of the homopolymers to that of the copolymer indicated that a molecular composite had been achieved according to the "rule of mixtures" [5]. However, a detailed morphological study directly examining the level of dispersion of the components in this material has not yet been carried out.

The goal of this study was to characterize with WAXS, SEM, and TEM the structure and morphology of the PBT/ABPBI triblock copolymer synthesized by Tsai et al. [8]. Additionally, structural and morphological results of this study on fiber and film of the PBT/ABPBI block copolymer were compared with the earlier results of a PBT/ABPBI physical blend (6,7).

*Figures are located at end of report.

SECTION II

BACKGROUND

1. PBT Fiber

PBT is a rigid-rod, extended chain, aromatic heterocyclic polymer with high strength, high modulus, and excellent environmental and thermal resistance. PBT has only on-axis bond rotations, resulting in extended rigid-rod molecules. Its chemical structure is shown in Figure 1. The unit cell structure was studied by Adams *et al.* [9], Roche *et al.* [10], and Odell *et al.* [11]. The non-primitive unit cell is monoclinic with the axis lengths of $a = 1.196$ nm, $b = 0.355$ nm, and $c = 1.235$ nm, and a unit cell angle of $\gamma = 100.9^\circ$ [10]. The PBT molecular axis is parallel to the c axis and molecules are located in the corners and center of the a - b plane of the unit cell. For an individual PBT molecule, the plane of the benzobisthiazole ring structure is -5° from the a axis and the phenylene plane is 25° from the a axis.

The morphology and properties of PBT fiber have been extensively studied [12-15]. Results from WAXS [15] and TEM [12-13] have shown that spun, drawn, and heat-treated PBT fiber has very high molecular and crystallite orientation. High molecular orientation and chain perfection was demonstrated from TEM selected area electron diffraction (SAED) results in which 27 orders of meridional reflections were observed [12]. High crystallite orientation was demonstrated from WAXS results in which a c -axis orientation factor of 0.99 was observed [14]. PBT molecules were generally found to be two-dimensionally (2-D)-ordered laterally and were axially disordered along the fiber axis [12], although limited 3-D ordering was occasionally observed [13] in TEM

lattice fringe images. Heat-treated PBT fiber contained crystallites with dimensions of about 20 nm along the c-axis, 9 nm along the a-axis, and 6 nm along the b-axis [7,12]. The high molecular and crystallite orientation along the fiber axis contributes to very high axial mechanical properties [12,14]. SEM images of a PBT fracture surface showed that the fiber has little ductility, in agreement with stress-strain curves which show linear elastic behavior to the fracture point [16]. Allen [15] studied the effect of heat treatment on as-spun PBT fiber and reported moduli up to 320 GPa and tensile strengths up to 3.1 GPa for the heat-treated fiber. The results of mechanical property studies on PBT, ABPBI, a 30% PBT/70% ABPBI physical blend, and a 30% PBT/70% ABPBI triblock copolymer are summarized in Table I.

2. ABPBI Fiber

ABPBI is an aromatic heterocyclic semi-flexible coil polymer with excellent thermal and mechanical properties [17]. Its chemical structure is shown in Figure 1. ABPBI can assume a coil-like structure due to off-axis rotations about its backbone bonds. It has not been studied as extensively as PBT and the unit cell of ABPBI has not been reported. However, the unit cells of polymers poly-2,6-benzothiazole (ABPBT) and poly-2,5-benzoxazole (ABPBO) have been reported to be orthogonal (pseudo-orthorhombic) by Fratini *et al.* [18]. On the basis of the similarity of the chemical structure of ABPBI to that of ABPBT and ABPBO, a preliminary crystal structure has been proposed for ABPBI with an orthorhombic unit cell with axis lengths $a = 0.72$ nm, $b = 0.35$ nm, and $c = 1.17$ nm [7].

The morphology of ABPBI has received limited study. It was found that stretching of ABPBI film caused negligible changes in d-spacings but produced higher orientation [7]. When as-spun fibers of ABPBI were heat treated, the length of the a axis was reduced from 0.83 nm to

0.72 nm due to improved lateral packing of chains. Krause *et al.* [7] found that the heat-treated fiber contained crystallites which had lateral dimensions no larger than 3 nm. Crystallites were three-dimensionally ordered within the fiber, but only two-dimensionally ordered at the fiber surface. Crystallites and molecules were moderately well-oriented with respect to the fiber axis. The molecular orientation was demonstrated from TEM SAED results in which 3 orders of meridional reflections were observed. The crystallite orientation was demonstrated from WAXS results in which a c -axis orientation factor of 0.91 was observed. SEM images of an ABPBI fiber fracture surface showed the presence of drawing and micronecking, which is in agreement with mechanical testing results which showed that ABPBI fiber had higher ductility (5.2%) and lower strength (1100 MPa) when compared to PBT (1.1% and 3100 MPa, respectively) [7]. This is due in part to the flexible-coil chain architecture of ABPBI and also the lower molecular and crystalline orientation in ABPBI fiber compared to PBT fiber. The mechanical properties of ABPBI have been studied by Hwang *et al.* [5] who reported a modulus of 36 GPa and a tensile strength of 1100 MPa for heat-treated fiber.

3. Polymer Phase Compatibility

Phase separation of the components of a polymer blend or a block copolymer can significantly affect mechanical properties. In macroscopic composite theory the effect of the geometry of the reinforcing phase can be evaluated in terms of a parameter known as the *aspect ratio*, defined as $2L/D$, where L is the length and D is the diameter of the reinforcing phase. High aspect ratios (preferably greater than 100) provide efficient reinforcement of matrix material by the reinforcing phase [19].

It has been proposed that the effect of reinforcement of a ductile polymer matrix by rigid-rod

molecules or rigid-rod molecular segments (of a copolymer) is analogous to the reinforcing effect of high aspect-ratio fiber on the properties of macroscopic composites [1,5]. If we consider, for example, that rigid-rod PBT molecules or molecular segments can be dispersed singularly or in small bundles ($<3\text{nm}$) in an ABPBI matrix, the aspect ratio of a PBT molecule or segment may be as high as 330, if the length and diameter are about 100 nm and 0.6 nm, respectively. Even for bundles of PBT molecules or segments 2 nm to 3 nm wide, an aspect ratio of 70 to 100 would be maintained and provide efficient reinforcement.

If, alternatively, rigid-rod molecules or molecular segments phase separate on a large scale from the flexible-coil matrix polymer, then the aspect ratio of the rigid-rod reinforcing phase would be reduced to a low value. A low aspect ratio and reduced amount of reinforcing component in the matrix would not be expected to provide efficient reinforcement.

Hwang *et al.* [5,20] investigated solution properties, processing, and mechanical properties of PBT/ABPBI physical blends in a solvent of methanesulfonic acid (MSA) and interpreted their results in terms of Flory's theory of phase equilibria of rigid-rod and flexible-coil polymer systems [21,22]. It was found from optical microscopy that when the total concentration (C) of the polymer in the solvent was above a critical concentration (C_{cr}), liquid crystalline domains formed in an optically isotropic liquid, demonstrating that the solution had phase separated. The critical concentration for phase separation varied from 2% to 6% polymer in solution as the ratio of PBT to ABPBI decreased. C_{cr} decreased when temperature decreased and when the molecular weight of PBT increased, in accordance with Flory's theory [22]. In another study of phase equilibria of a block copolymer, Tsai *et al.* [8] found that the critical concentration was 5.8% for phase separation of a 30% PBT/70% ABPBI triblock copolymer in MSA compared to 3% for phase separation of a 30% PBT/70% ABPBI physical blend in MSA. This shows that phase

separation was inhibited by combining PBT and ABPBI in the form of a copolymer rather than in the form of a physical blend.

4. Physical Blend Cast Film

The effect of phase separation on the morphology of a physical blend of 30% PBT/70% ABPBI has been studied by Hwang et al. [5] and Krause et al. [7]. SEM images of PDIAB/ABPBI or PBT/ABPBI vacuum cast films showed brittle, 0.1 μm to 4 μm long, ellipsoidal particles separated from the adjacent ductile matrix material. The removal of solvent during the casting process caused the polymer concentration to rise above C_{cr} and induce thermodynamically favored phase separation in the binary rod/coil blend [22]. The liquid crystal phase separation was manifested in the solid state by the formation of elongated second-phase particles 0.1 μm to 4 μm in length. SEM backscattering studies of the films showed that the ellipsoidal particles were composed chiefly of sulfur-rich PBT. The ellipsoidal particle shape was expected since the geometry of the rod-like PBT molecules would cause them to align side by side in elongated liquid crystalline domains during phase separation. This was confirmed by Krause and Adams [6] who reported that the particles were chiefly composed of aggregates of 10-nm PBT crystallites moderately well-aligned with the longitudinal axis of the ellipsoids. The matrix material was ductile and composed chiefly of ABPBI. Figure 2a shows a schematic representation of the phase-separated PBT-rich particles in the ABPBI-rich matrix. As listed in Table I, the modulus is 1.1 GPa and tensile strength is 35 MPa. These values are roughly 1 order of magnitude less than ABPBI fiber and 2 orders of magnitude less than PBT fiber. These very low properties, compared to the homopolymer fiber, are due to phase separation, random orientation, and poor adhesion of the PBT-rich particles to the ABPBI-rich matrix.

5. Physical Blend Spun Fiber

The effect on properties and morphology of processing a 30% PBT/70% ABPBI physical blend by dry-jet/wet spinning has been studied by Hwang *et al.* [5] and Krause *et al.* [7]. SEM images of a fiber fracture surface showed reduced fibrillation (compared to PBT fiber) and no phase separation to the 20-nm resolution limit of the instrument. WAXS and TEM showed that heat-treated fiber contained well-oriented molecules crystallites of both ABPBI and PBT which were less than 3 nm in width. The ABPBI molecules and crystallites were more oriented in the blend fiber than in the pure ABPBI fiber due to enhanced orientation of ABPBI molecules by entanglement with PBT molecules. PBT molecules and crystallites were less oriented in the blend fiber than in pure PBT fiber due to the ABPBI molecules that inhibited orientation. Crystallites of PBT and ABPBI were less than 3 nm in size as a result of immobilization of the entangled and dispersed PBT and ABPBI molecules during rapid coagulation of the homogeneous solution in the fiber spinning process. Individual molecules of crystallites of PBT less than 3 nm in lateral size may have been present in the fiber, but their presence could not be determined from TEM. Since the aspect ratio of the reinforcing phase of PBT molecules or molecular bundles was very high it was stated that a molecular composite had been achieved. Figure 2b shows a model of the morphology of the physical blend molecular composite. Good dispersion, excellent adhesion, and high orientation of PBT in ABPBI gave efficient reinforcement which resulted in high values of mechanical properties in the molecular composite fiber, especially when compared to the phase-separated film. Properties are listed in Table 1.

In the physical blend system the "molecular composite" fiber ($C < C_{cr}$) had values of strength and modulus which were roughly one order of magnitude greater than the physical blend phase-separated fiber (values appear in reference [7]) and two orders of magnitude greater than

the phase-separated ($C > C_{cr}$) film. The modulus of the "molecular composite" fiber is about one-third of that of pure PBT fiber, which corresponds reasonably well to the "rule of mixtures" for a uniaxially reinforced composite. However, the use of the "rule of mixtures" has been based upon the measured, not the theoretical, modulus of PBT which raises questions as to the applicability of the "rule of mixtures" for molecular composites. This question will be considered further in the discussion of results in this study. The tensile strength is only slightly more than that of the ABPBI fiber, but tensile strength is strongly dependent on flaws and processing variations which may have limited possible improvements.

The value of elongation to break for the "molecular composite" fiber is reduced to about one-quarter of that for the phase-separated film. This occurs both because phase separation of PBT gives a larger fraction of ductile ABPBI in the matrix and because high orientation of molecules in the "molecular composite" fiber limits elongation prior to fracture.

6. Copolymer Film and Fiber

Also included in Table I are the mechanical property results of the 30% PBT/70% ABPBI block copolymer from Tsai et al. [8]. Mechanical properties of copolymer fiber spun from homogeneous solution ($C < C_{cr}$) are similar to those of physical blend ($C < C_{cr}$) fiber, which makes it likely that a molecular composite fiber has formed. The slightly higher (30%) strength of the copolymer fiber may be due to processing differences or structure and morphology differences. Modulus and strength of the copolymer fiber are roughly one order of magnitude larger than the copolymer film vacuum cast from a phase-separated solution ($C > C_{cr}$). The elongation to break is much greater for the copolymer film than the fiber. The significance of this and other mechanical property results will be discussed and correlated to morphological results later in this report.

Table I
Mechanical Testing Results

<u>Sample</u>	<u>Modulus</u>		<u>Tensile Strength</u>		<u>Elongation to Break</u>
PBT fiber	320	GPa	3100	MPa	1.1 %
	47	Mpsi	460	ksi	
ABPBI fiber	36	GPa	1100	MPa	5.2 %
	5.3	Mpsi	160	ksi	
30% PBT/70% ABPBI C>C _{cr} blend film	1.1	GPa	35	MPa	5.6 %
	0.16	Msi	5.1	ksi	
30% PBT/70% ABPBI C<C _{cr} blend fiber	120	Gpa	1300	MPa	1.4 %
	17	Msi	180	ksi	
25% PBT/75% ABPBI C>C _{cr} copolymer film	2.4	Gpa	220	MPa	43 %
	0.35	Msi	32	ksi	
30% PBT/70% ABPBI C<C _{cr} copolymer fiber	100	GPa	1700	MPa	2.4 %
	15	Msi	250	ksi	

SECTION III

EXPERIMENTAL METHODS

1. Materials Processing

The synthesis of PBT/ABPBI triblock copolymers has been described by Tsai *et al.* [8]. ABPBI monomer was reacted from the ends of PBT molecules to form triblock copolymer molecules such that the molar ratio of the two components along a given molecule was 35% ABPBI / 30% PBT / 35% ABPBI. This was referred to as a 30% PBT/ 70% ABPBI block copolymer. The molecular weight for the original PBT block component was estimated by intrinsic viscosity measurements to be 41 kg/mole. The length of the PBT segment and of each of the ABPBI segments is about 100 nm.

The techniques for processing the copolymer into fiber and film were reported previously by Hwang *et al.* [5]. A mixture of 97.5 vol% methanesulfonic acid (MSA) and 2.5 vol% chlorosulfonic acid (CSA) was the solvent for the polymers. The critical concentration of the copolymer in the solvent was 5.8 wt%.

Fiber was spun by extruding $C < C_{cr}$ solution through a spinneret die into a water coagulating bath. The fiber was dry-jet/wet-spun to a high draw ratio in the air gap between the die and the water bath. The wet fiber was neutralized in NH_4OH overnight, rinsed in distilled water, and heat-treated under tension at elevated temperatures in air.

The processing of vacuum cast film has been described by Husman *et al.* [2]. Solvent from a $C < C_{cr}$ solution was removed in a sublimator, with the slowly decreasing amount of solvent resulting in a concentrated ($C > C_{cr}$) solution and, ultimately, a cast film. The film was neutralized, rinsed, and dried in a vacuum oven to remove residual solvent.

2. Scanning Electron Microscopy

Samples were prepared for SEM imaging by submerging fiber and film in liquid nitrogen and then fracturing. The fracture surfaces were sputter-coated with gold-palladium to prevent charging during imaging and were examined on an ISI Alpha 9 SEM at 10KV at magnifications from 100X to 10,000X. Images were recorded on Polaroid P/N 55 film.

3. Wide Angle X-ray Diffraction

The fiber sample was prepared for WAXD by winding approximately 10 cm of a single filament around a cardboard holder. The film sample for WAXD required no special preparation techniques. The WAXD photographs were recorded with flat-film Statton (Warhus) cameras. CuKalpha radiation was generated by an Elliot GX20 rotating anode x-ray generator with a nickel filter. The sample-to-film distances were 29.2 ± 0.2 mm for the two Statton cameras, calibrated by the known crystalline reflections of a standard silicon powder, SRM 640.

4. Transmission Electron Microscopy

TEM samples were prepared by ion thinning since copolymer film and fiber were not amenable to preparation by more traditional detachment replication techniques [12]. In ion-thinned samples damage occurred at the thinnest edges of some sample areas due to the bombardment of the copolymer with argon ions. Many undamaged areas were, however, available for examination. TEM images and SAED patterns were taken on Kodak SO-163 film on a JEOL 100CX at an accelerating voltage of 100 kV using low-dose techniques.

SECTION IV

RESULTS AND DISCUSSION

1. Scanning Electron Microscopy

a. Cast Copolymer Film

The fracture surface of the 30% PBT/70% ABPBI $C > C_{cr}$ vacuum cast copolymer film is shown in Figure 3a at lower magnification and in Figure 3b at higher magnification. The fracture surface at low magnification is flat and rather "spotty." At higher magnification the "spots" are actually seen to be a combination of particles, rows of particles, and some small platelets embedded with the matrix material. There is a great deal of fine scale micronecking on the larger, rather flat surfaces. Frequently, micronecks are terminated by a small particle or a small line of particles.

In previous studies [5,7] on phase-separated film and fiber of a 30% PBT/70% ABPBI physical blend, SEM images showed 0.1 to 4- μ m particles separated from the matrix which resemble the particles observed here. However, the particles in the block copolymer show much better adhesion to the matrix than the particles in the cast film of the physical blend. In the copolymer this is due to the chemical bond between the PBT molecular segments in the particles and ABPBI molecular segments in the matrix; whereas in the physical blend there is evidently only a mechanical bond between the PBT in the particles and the ABPBI in the matrix. In the physical blend such particles were identified as phase-separated material composed chiefly of PBT crystallites. In the block copolymer, TEM results presented later also show that the small particles

are composed chiefly of phase-separated PBT crystallites. This is reasonable since the PBT molecular block segments are about 0.1 μm long. Although phase separated particles in the physical blend film grew to as large as 4- μm -long ellipsoids, it is highly unlikely that the particles in the copolymer film could grow much larger in length than 0.1 μm since the end of each 0.1- μm PBT segment is terminated with a flexible-coil ABPBI segment. It might, however, be possible for the rigid-rod PBT molecular segments to phase-separate and coalesce with lateral growth between adjacent rod segments. There are indications that this occurred since either small platelets or strings of 4 to 5 phase-separated particles up to 0.4 μm in width are occasionally observed. A model for the morphology of phase-separated material in the cast copolymer film is shown in Figure 5a.

In the previous study on the phase-separated physical blend film it was also shown that the matrix material was composed chiefly of ABPBI [7]. It is likely that the matrix in the phase-separated copolymer film is also chiefly ABPBI. This is indicated by the ductile fracture behavior, which is characteristic of ABPBI, of the matrix adjacent to the phase-separated particles and platelets. Large-scale 0.5 to 1- μm -necking, which was observed for the phase-separated physical blend film, is unlikely to occur with the copolymer film since the flexible-coil segments of the triblock copolymer molecules only extend a maximum of about 0.1 μm from each end of the PBT segment. In the phase-separated form it is thus unlikely that ABPBI in the block copolymer extends continuously beyond 0.1 μm to 0.3 μm . This accounts for the small-scale micronecking observed here.

b. Spun Copolymer Fiber

The fracture surface of the 30% PBT/70% ABPBI $C < C_{\text{cr}}$ spun fiber is shown in Figure

4a at low magnification and in Figure 4b at higher magnification. The low-magnification image shows that the fiber has split through the middle parallel to the fiber axis. This indicates that there is at least moderate orientation of the molecules along the fiber axis. Data presented later in this study indicate that the molecules and crystallites are well-oriented along the fiber axis. The fracture surface itself is rather flat and approximately perpendicular to the fiber axis. It is somewhat unusual that there is high molecular orientation and yet a flat fracture surface across the fiber, with little or no longitudinal fibrillation. This indicates that although there is high axial strength along the fiber, there is also moderate lateral strength across the cross section of the fiber which would inhibit fibrillation. The structure of the fracture surface contrasts sharply with the structure observed in other types of high-strength, high-modulus fibers. PBT fiber fibrillates extensively upon fracture, as expected, due to its high axial strength and low lateral strength [12]. The 30% PBT/70% ABPBI physical blend fiber, which has relatively high strength, fibrillates moderately upon fracture, but to a more limited extent than PBT, due to its moderate ductility and lateral strength. On the other hand, ABPBI fiber, whose strength and modulus are about an order of magnitude lower than that of PBT, fibrillates little upon fracture, as expected, both due to reduced orientation and moderately high ductility and lateral strength. Thus, it appears that the lack of fibrillation in the 30% PBT/70% ABPBI copolymer fiber is an indication that, if the orientation is similar to that of the 30% PBT/70% ABPBI physical blend fiber, it has greater ductility and higher lateral strength than the physical blend fiber.

The higher magnification image of the copolymer film in Figure 4b shows unusual and significantly different morphological features in the skin region near the fiber surface compared to the core region near the center of the fiber. The skin region is composed of solid material while the interior region has elongated voids running along the fiber axis. It is likely that the voids are a result of the fiber-spinning process. The diameter of the fiber of 60 to 70 μm is larger than that

currently used, and may have induced void formation during spinning. It may also be that residual solvent in the core left voids behind after being removed. It is important to note here that since the voids occupy about 35% of the cross-sectional area, it is likely that the mechanical properties of the fiber would be more than 50% higher than those measured if the fiber had been free of voids.

Morphology and property differences between the fiber surface and the fiber interior are frequently referred to as a skin-core effect. A skin-core effect exists for many ordered polymer fiber systems, including PPTA [23,24], PBT [12], and ABPBI [7]. The role of the skin-core structure in mechanical behavior of fiber is not at all well-understood, but it may have a significant effect on properties, especially in composite applications.

Figure 4a shows that, along the length of the skin, there are longitudinally aligned layers with sharp boundaries which are interconnected in a region between the surface and about 5 to 10 μm into the interior. There are steps at the boundaries of these layers which range in height from about 0.1 μm to greater than 5 μm . The fracture surface on top of some of these layers is flat or stepped while on other surface areas it shows considerable micronecking. Upon closer inspection it is seen that even the flattest surface areas exhibit some extremely fine micronecking. The presence of the limited to moderate micronecking indicates that the fiber has moderate ductility.

The fiber interior contains elongated voids which are 1 μm to 5 μm long and decrease in size from about 1 μm to 3 μm at the center of the fiber to about 0.2 μm to 0.5 μm in diameter towards the skin. As with the morphology of the fracture surface in the skin region, the fracture surface in the interior region is generally flat, but upon closer inspection many regions appear to have a significant amount of shallow micronecking. The step structure is also present here with steps

ranging in size from a fraction of a micron to 2 μm to 3 μm . The origin of the step structure is unclear.

The fiber, unlike the vacuum cast film does not appear to contain any phase-separated particles to the 20-nm resolution limit of the SEM. However, it may be difficult to distinguish between very fine particles on the surface and very fine micronecking. It is reasonable to place an initial upper size limit of 20 nm, as determined by SEM, on any possible phase separation in the copolymer fiber which has been processed from homogeneous solution. A similar conclusion was reached for SEM studies of 30% PBT/70% ABPBI physical blend fiber spun from a homogeneous solution [5,7]. The question of phase separation will receive additional consideration in the section on TEM studies.

2. Wide Angle X-ray Scattering

To compare the structure of samples in this study with that of samples from a previous study [7], the WAXS photographs have been included in Figure 6 for a) PBT fiber, b) ABPBI fiber, and c) spun fiber and d) cast film of a 30% PBT/70% ABPBI physical blend. The d-spacings in Table II were determined from the reflections in the photographs.

a. Cast Copolymer Film

The WAXS pattern for 30% PBT/70% ABPBI $C > C_{cr}$ vacuum cast film is shown in Figure 6e. There are four uniform Debye rings present. The 0.58-nm reflection, which corresponds to an equatorial spacing in PBT fibers, indicates PBT crystallites are present. The 0.35-nm reflection can be a combined reflection for both PBT and ABPBI, although it is only

certain that PBT crystallites are present from the 0.58-nm reflection. Additionally, there are 1.25-nm and 0.42-nm reflections which correspond to meridional spacings in pure PBT fibers. The slightly arced rings indicate there is slight overall orientation of crystallites in the film. The equatorial reflections from crystallites in the film are moderately sharp, which indicates crystallites are of an intermediate size. There are no reflections present which are characteristic of ABPBI crystallites. The results are similar to those observed for the WAXS of the vacuum cast film of the 30% PBT/70% ABPBI physical blend shown in Figure 6c.

TABLE II
The d-spacings (nm) from WAXD Patterns*

30% PBT/70% ABPBI						
	PBT fiber	ABPBI fiber	Physical Blend		Copolymer	
			C>Ccr film	C<Ccr fiber	C>Ccr film	C<Ccr fiber
Equatorial (hk0) d-spacings	--	--	--	--	--	1.28
	--	0.72	0.83	0.74	--	0.80
	0.58	--	0.60	0.61	0.58	0.63
	--	0.45	--	--	--	--
	0.35	0.35	0.35	0.35	0.36	0.36
	0.32	--	--	--	--	--
Off-axis (hkl) d-spacings	0.30	--	--	--	0.28	--
	--	0.51	--	--	--	--
	--	0.43	--	--	--	--
	--	0.32	--	--	--	--
Meridional (00l) d-spacings	1.25	--	--	1.27	1.25	1.27
	--	(1.17)	--	--	--	--
	0.63	--	--	0.60	--	0.60
	--	0.58	--	--	--	--
	0.42	--	0.42	0.42	0.42	0.42
	--	0.39	--	0.39	--	0.39
	0.31	--	--	0.31	--	0.31
	--	0.29	--	--	--	0.29
	0.24	--	0.25	0.25	--	--
	--	(0.23)	--	0.23	--	--

*Values in parentheses are calculated, not measured.

b. Spun Copolymer Fiber

The WAXD pattern for 30% PBT/70% ABPBI $C < C_{cr}$ fiber shown in Figure 6f shows highly-arc'd equatorial reflections, indicating well-oriented crystallites, and flat meridional reflections, sometimes in pairs, extending out to high orders, indicating well-oriented molecules of both species. This copolymer fiber has equatorial and meridional spacings present which correspond to those in both PBT and ABPBI fibers. The 0.80-nm equatorial reflection, a characteristic ABPBI equatorial reflection in heat treated fiber, indicates ABPBI crystallites are present. Additionally, there are at least two meridional reflections present (at 0.39 nm, and 0.29 nm) which are characteristic ABPBI meridional spacings. This indicates that molecules of ABPBI are well-ordered and moderately oriented in the blend fiber. In fact, the meridional reflections characteristic of ABPBI in the blend fiber are flatter and sharper than those in pure ABPBI fiber. The physical blend fiber also displayed similar WAXS features. Hwang et al. [5] have attributed higher orientation of the ABPBI molecules in a physical blend spun fiber to entanglement of ABPBI with PBT which extends ABPBI molecules along the well-oriented PBT molecules resulting in higher orientation of the ABPBI molecules. The higher orientation of the ABPBI molecules in the block copolymer than in pure ABPBI fiber is also probably due to entanglement and extension of ABPBI with PBT which results in higher orientation of the ABPBI molecules. Although the alignment of ABPBI molecules and crystallites increases in the copolymer fiber, the diffuseness of the characteristic 0.74-nm and 0.44-nm reflections indicates crystallite size remains relatively small.

The 0.63-nm spacing, a characteristic PBT equatorial reflection, indicates PBT crystallites are present. Additionally, there are four meridional reflections (1.27-nm, 0.604-nm, 0.420-nm, 0.31-

nm) which are characteristic PBT meridional reflections. This indicates that the molecules of PBT are well-oriented in the copolymer fiber. However, as with the blend fiber, there are not as many orders of meridional reflections, nor are the characteristic PBT meridional reflections as flat or as sharp as those in the pure PBT fiber which indicates that PBT molecules are less oriented than in pure PBT fiber. This is probably due to the presence of semi-flexible coil ABPBI molecular segments which inhibit orientation of rigid-rod PBT molecules during the spinning of copolymer fiber. Also, the solution is not spun from a nematic liquid crystal state as it is in spinning of pure PBT fiber.

A major difference between the PBT in the copolymer fiber and the pure PBT fiber is the relative diffuseness of the characteristic 0.58-nm PBT reflection and the composite 0.35-nm reflection. The diffuseness of these reflections indicates that the crystallite size for PBT is much smaller in the copolymer fiber than in the pure PBT fiber. This small crystallite size is a result of the processing conditions in which there is no large-scale phase separation in the $C < C_{cr}$ solution prior to fiber spinning. After spinning and during coagulation large-scale phase separation of PBT from ABPBI is inhibited by the entangled of ABPBI molecules which also inhibits growth of larger or more-ordered PBT crystallites.

There is another interesting trend present in the data. One of the characteristic PBT equatorial reflections and one of the characteristic ABPBI equatorial reflections increase in value when considering first the sample of pure PBT or pure ABPBI, then the physical blend $C < C_{cr}$ spun fiber, and finally the copolymer $C < C_{cr}$ spun fiber. The characteristic ABPBI spacing increases from 0.716 nm to 0.737 nm to 0.797 nm as the samples progress from pure ABPBI, to ABPBI in physical blend fiber, to ABPBI in copolymer fiber. This indicates that the edges of the planes of the heterocyclic rings in the unit cell are being pushed further apart laterally. In the physical blend

fiber it is likely that the increase in the spacing is due to some mixing of PBT molecules in the ABPBI crystal which perturbs the lattice. In the copolymer fiber the spacing of the planar edges of the heterocyclic rings is even larger and there is evidently more mixing of PBT molecules in the ABPBI crystallites and greater perturbation of the lattice.

A similar trend is observed for the characteristic PBT spacing which increases from 0.579 nm to 0.611 nm to 0.634 nm as the samples progress from pure PBT, to PBT in the physical blend fiber, to PBT in the copolymer fiber. It appears that ABPBI is probably mixing in the crystallites of PBT, thus perturbing the lattice and increasing spacing of the planar edges of the heterocyclic rings. Only a very small increase in spacings occurs for the 0.35-nm reflection which is the planar spacing between the planes of the heterocyclic rings in both PBT and ABPBI crystallites. This indicates that any mixing of the ABPBI in PBT crystallites occurs chiefly at the edges of the planes of the heterocyclic rings rather than between the planes of the heterocyclic rings. The same conclusion would also hold true for PBT mixing with ABPBI crystallites. Overall, the larger increase in d-spacing of both PBT and ABPBI at the edges of the planes of the heterocyclic rings of the block copolymer compared to the physical blend indicates that molecules are mixing more intimately in the copolymer than in the polymer blend.

3. Transmission Electron Microscopy

a. Cast Copolymer Film

Figure 7a is a dark field image of an ion-thinned section of the cast copolymer film. There are a few regions in white that are about 100 nm thick and 100 nm to 200 nm wide. Each region is composed of much smaller white "flakes" which are crystallites. These crystallites have sizes on the order of 10 nm.

A typical SAED pattern for a larger 5 μm diameter area of electron beam illumination is shown in Figure 7b in the lower left corner of the micrograph. This larger area SAED pattern shows that there is no overall orientation of crystallites within the film. However, when an SAED pattern is obtained from a 0.1- μm area within a particle, as shown in Figure 7c on the lower right side, it contains relatively sharp and moderately well-arc'd equatorial reflections with spacing ratios characteristic of PBT, indicating that there are large, moderately well-oriented PBT crystallites within the particles. Several orders of fairly sharp, but slightly curved, meridional reflections are present, indicating moderate molecular orientation. The meridional (001) spacing of PBT was used as a standard to calculate the d-spacings of the equatorial reflections. The presence of the 0.60-nm reflection confirms that crystallites are PBT. This agrees with the SEM results which showed that the 0.1- μm particles seen here in dark field imaging are composed chiefly of PBT. Additionally, it has been found from the orientation of the diffraction pattern that the chain axis of the PBT molecules and c -axis of the crystallites are aligned perpendicular to the wider dimension of the platelets and particles.

From the above results, it is concluded that 30% PBT/70% ABPBI C>C_{cr} copolymer film

contains phase-separated particles within a ductile matrix. These particles are chiefly composed of a lateral agglomeration of moderately oriented 8 to 10-nm-wide PBT crystallites. This supports the model for the morphology of the cast copolymer film shown in Figure 5a.

b. Spun Copolymer Fiber

The TEM dark field image from the (hk0) reflections of the fiber spun from 30% PBT/70% ABPBI $C < C_{cr}$ solution is shown in Figure 8a. There are no obviously discernable features greater than 3 nm in size. From this observation and limitations of the statistical resolution of the image, it can be concluded that the size of any crystallites that are present would have to be about 3 nm or less.

Figure 8b shows the SAED pattern for $C < C_{cr}$ fiber. It contains a broad moderately well-arc'd equatorial reflection at 0.84 nm. This indicates that ABPBI crystallites are present, but that they are very small and/or disordered with a size of 3 nm or less.. This is in agreement with the dark field results. The 0.35-nm reflection is a composite reflection for PBT and ABPBI structures. It indicates that PBT and/or ABPBI crystallites may be present. The moderate arcing of the equatorial reflections indicates moderate crystallite orientation along the fiber axis. The above SAED results are similar to WAXS results which also indicate the presence of small and/or disordered crystallites which are moderately oriented. The broad and somewhat curved meridional reflections indicate that there is also good orientation of the molecules with respect to the fiber axis. The presence of three meridional orders characteristic of ABPBI meridional reflections indicates that the ABPBI molecules are well-enough oriented and ordered to produce meridional reflections. Although the diffuseness of the pattern makes measurement of spacings

difficult, there are clearly two distinct sets of meridional spacings present. Measurement of the spacings indicates that oriented molecules of both PBT and ABPBI are present.

It is concluded from the dark field images and SAED patterns that 30% PBT/70% ABPBI $C < C_{cr}$ copolymer fiber contains small, moderately well oriented crystallites of PBT and ABPBI which are no larger than 3 nm in diameter. The TEM images show that no crystalline phase separation occurs at a scale larger than 3 nm for either the fiber or the film. The PBT and ABPBI components have been dispersed at a scale finer than 3 nm. Thus, a molecular level composite has been formed in the copolymer fiber. A model for the morphology of the "molecular composite" copolymer fiber is shown in Figure 5b.

4. General Discussion

When copolymer film is vacuum cast from 30% PBT/70% ABPBI $C > C_{cr}$ solution, SEM and TEM images show phase separation occurs and platelets and particles, 0.1 to 0.4 microns are formed. TEM reveals that these phase-separated particles are composed of crystallites which are about 8 to 10 nm in size, and SAED indicates the crystallite c axis and molecules are oriented perpendicular to the width of the platelet.

It can be concluded that the crystallites in the particles are chiefly PBT. First, SAED patterns reveal crystallites of PBT present in the particles. It is unlikely that there are crystallites of ABPBI present within the particles. Flory's theory of rigid-rod phase equilibria [21,22] actually predicts total exclusion of the flexible molecules from the rod-rich phase, but it may, however, be possible that some ABPBI exists within the particles as a non-crystalline material.

The matrix is chiefly composed of ABPBI since there is less PBT than ABPBI in the total sample (30% PBT/70% ABPBI) and relatively little PBT would be left in the matrix material if the particles are mostly PBT. The matrix of the phase-separated film showed some ductility in SEM photos similar to the ductility observed in SEM photos of fractured ABPBI fibers. This is probably due both to the lack of orientation and the reduced amount of PBT in the matrix. Thus, these data indicate the matrix is chiefly ABPBI. This is in agreement with Flory's theory which predicts some, but little, rigid-rod polymer will still be present in the coil phase.

The modulus and strength of the phase separated material is also relatively low because of the low aspect ratio of the PBT-rich particles which results in inefficient reinforcement of the matrix material. However, the mechanical properties are higher than those for the vacuum cast film of the physical blend. This is probably due to the smaller particles from reduced phase separation and improved adhesion between phases in the vacuum cast copolymer film.

When copolymer fiber is spun from 30% PBT/70% ABPBI $C < C_{cr}$ solution no large-scale phase separation is observed. The SAED and WAXS patterns indicate that both PBT and ABPBI crystallites are present. TEM dark field images reveal no features present at a scale larger than 3 nm, demonstrating that a dispersion of PBT in ABPBI at a molecular level of 3 nm or better has been achieved. Stated more conservatively, it can be said that no crystalline phase separation occurs at a scale larger than 3 nm. A copolymer coil/rod/coil with this level of dispersion is considered to be a molecular composite. Crystallites of PBT segments less than 3 nm in lateral size may be present in the molecular composite, but this cannot be determined from TEM. Thus, the aspect ratio of the reinforcing phase of PBT molecular segments and molecular segment bundles is very high in the molecular composite fiber compared to the PBT in particles in the phase-separated film. This results in more efficient reinforcement of the matrix. In the copolymer

molecular composite fiber, SAED patterns show that the PBT and ABPBI molecules and crystallites are also moderately well-oriented. Both efficient reinforcement and orientation of ABPBI and PBT result in high values of mechanical properties in the copolymer molecular composite fiber. The values of its modulus and strength are, respectively, 43 and 8 times greater than those of the phase-separated film.

The value of elongation to break for the copolymer molecular composite fiber (2.4%) is dramatically reduced, by a factor of about 20, compared to that for the phase-separated copolymer film (43%). This occurs because most of the reinforcing PBT has phase-separated out of the matrix material in the phase-separated film, thus giving the matrix material a larger fraction of the more ductile ABPBI. Interestingly, the elongation to break is 8 times higher for the cast copolymer film compared to the cast physical blend film. This is evidently due to the reduced scale of phase separation and the improved adhesion between the matrix and the particles in copolymer film.

There are some additional comparisons that can be made between the "molecular composite" fibers of the copolymer and the physical blend with respect to the mechanical properties of the PBT homopolymer fiber. Since, in general, elongation to break decreases with increasing fiber orientation, it can be considered a crude measure of orientation of crystallites and molecules within the fiber. The elongation to break in the physical blend fiber is 1.4% compared to 1.1% in the PBT fiber. This indicates that it might be possible to slightly improve the orientation in the physical blend fiber. However, in the copolymer fiber the elongation to break is 2.4%, more than double that for the PBT fiber. This indicates that it might be possible to moderately increase the orientation of the copolymer fiber and achieve corresponding increases in modulus and tensile strength. Also, since the SEM micrograph of the copolymer fiber showed 30% to 40% voids in

the fiber interior, the mechanical properties could actually be increased by more than 50% for a void-free fiber. Thus, it is not unreasonable to project that, with optimum processing conditions, the modulus and tensile strength of the copolymer fiber could be increased by a factor of 1.5 to 2.

A doubling of the modulus would, of course, significantly exceed the modulus predicted by the "rule of mixtures" for uniaxially reinforced composites. However, the application of the "rule of mixtures" has been assumed to be a simplified approach based on the measured values of properties of the component materials, not the theoretically predicted values. The theoretically predicted value of the modulus of PBT is 615 GPa, almost double the value of the highest measured modulus [25]. By applying the theoretical modulus to the "rule of mixtures" for the 30%PBT/70%ABPBI copolymer fiber, it should be possible, with perfect orientation, to achieve a modulus of about 180 GPa, which is double the currently measured value and almost equal to the value of steel. This would yield a specific modulus about eight times that of steel. The potential for superior mechanical properties of copolymer molecular composites is excellent, but additional work is necessary for optimizing processing conditions and for improved modeling for property prediction.

SECTION V

SUMMARY AND CONCLUSIONS

SEM, TEM, and WAXD were used to examine the structure and morphology of fiber and film of a 35%ABPBI/30%PBT/35%ABPBI triblock copolymer processed under different conditions.

When copolymer was vacuum cast from a $C > C_{cr}$ solution, a film formed which contained 0.1 to 0.4 micron wide platelets and particles in a ductile matrix. The platelets and particles were composed chiefly of an aggregation of 8 to 10-nm PBT crystallites with the c -axis and the molecular axis moderately oriented perpendicular to the width of the platelets and particles. The matrix material was composed chiefly of ABPBI. Low values of modulus and strength of the film were due to phase separation of the PBT molecules from the matrix material. The values of modulus, strength, and elongation-to-break were all higher for the vacuum cast copolymer film compared to a physical blend cast film due to reduced phase separation and improved adhesion between the matrix and the particles.

Heat-treated copolymer fiber dry-jet/wet-spun from an optically homogeneous ($C < C_{cr}$) solution exhibited no large scale phase separation. Phase separation was inhibited by rapid water coagulation of fiber during the spinning process. The heat-treated fiber contained well-oriented, two-dimensionally ordered crystallites of both PBT and ABPBI. The crystallites had lateral dimensions no larger than 3 nm, demonstrating that the PBT molecular segments were well-dispersed and that a rigid-rod molecular composite had been achieved.

In the molecular composite fiber, the fine dispersion and high orientation of the rigid-rod PBT molecules efficiently reinforced the matrix material resulting in high values of mechanical properties. The strength (1700 MPa) and modulus (100 GPa) were, respectively, 8 and 26 times greater than those of the cast copolymer film. The modulus was approximately equal to that predicted by the "rule of mixtures" based on the measured modulus of PBT fiber, but it is likely that processing improvements could double the modulus, which suggests that the "rule of mixtures" should be based on the theoretically predicted modulus of PBT.

REFERENCES

1. T. E. Helminiak, C.L. Benner, F.E. Arnold, G.E. Husman, U.S. Pat. Appl. 902,525 (1978).
2. G. Husman, T. Helminiak, W. Adams, D. Wiff and C. Benner, *Am. Chem. Soc. Symp. Ser.*, **132**, 203 (1980).
3. M. Takayanagi, T. Ogata, M. Morikawa, and T. Kai, *J. Macromol. Sci. Phys.*, **B17**, 519 (1980).
4. M. Takayanagi, *Pure and Appl. Chem.*, **55**, 819 (1983).
5. W-F. Hwang, D. R. Wiff, C. L. Benner and T. E. Helminiak, *J. Macromol. Sci. Phys.*, **B22**, 231 (1983).
6. S. J. Krause and W. W. Adams, *Proceedings, 41st EMSA Meeting*, San Francisco Press, San Francisco, 1983, p. 32.
7. S. J. Krause, T. Haddock, G. E. Price, P. G. Lenhert, J. F. O'Brien, T.E. Helminiak, and W. W. Adams, *J. Polymer Sci. - Polymer Physics Edition*, **24**, 1991 1986.
8. T. T. Tsai, F. E. Arnold, and W. F. Hwang, *Am. Chem. Soc. Poly. Preprints*, **26**, 144 (1985).
9. W. W. Adams, L. V. Azaroff, and A. K. Kulthreshthra, *Z. Kristal.*, **150**, 321 (1980).
10. E. J. Roche, T. Takahashi and E. L. Thomas, *Am. Chem. Soc. Symp. Ser.* **141**, 303 (1980).
11. J. A. Odell, A. Keller, E. D. T. Atkins and M. J. Miles, *J. Mater. Sci.*, **16**, 3309 (1981).
12. J. R. Minter, K. Shimamura, and E.L. Thomas, *J. Mat. Sci.*, **16**, 3303 (1981)
13. K. Shimamura, J. R. Minter and E. L. Thomas, *J. Mater. Sci. Lett.*, **2**, 54 (1983).
14. S. R. Allen, R.J. Farris, and E.L. Thomas, *J. Mat. Sci.*, **20**, 4583 (1985).
15. S. R. Allen, R.J. Farris, and E.L. Thomas, *J. Mat. Sci.*, **20**, 2727 (1985).
16. L. Feldman, R.J. Farris, and E.L. Thomas, *J. Mat. Sci.*, **20**, 2719 (1985).
17. T. E. Helminiak, *Am. Chem. Soc. Org. Coat. Plast. Chem.*, **40**, 475 (1979).
18. A. V. Fratini, E. M. Cross, J. O'Brien and W. W. Adams, *J. Macromol. Sci. Phys.*, **B24**, 159 (1985-1986).

REFERENCES (Concluded)

19. R. M. Christensen, *Mechanics of Composite Materials*, Wiley, New York, 1979, pp. 89-99.
20. W-F. Hwang, D. R. Wiff, C. Verschoore, G. E. Price, T.E. Helminiak and W. W. Adams, *Polym. Engr. & Sci.*, **23**, 784 (1982).
21. P. J. Flory, *Proc. Roy. Soc. London*, **A234**, 73 (1956).
22. P. J. Flory, *Macromolecules*, **11**, 1138 (1978).
23. M. G. Northolt and J. J. van Aartsen, *J. Poly Sci: Polymer Symposium*, **58**, 283-296 (1977).
24. L.S. Li, L.F. Allard, and W.C. Bigelow, *J. Macromol. Sci. Phys.*, **B22**, 269 (1983).
25. J. Stewart, private communication.

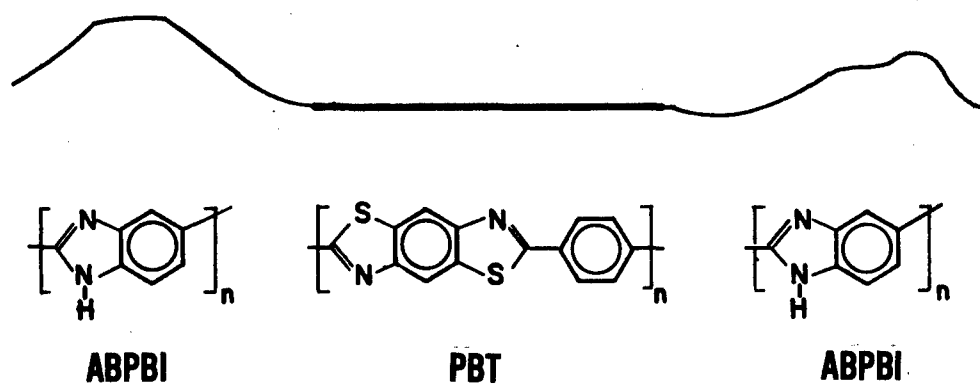


Figure 1. Chemical and Molecular Structure of a PBT/ABPBI Triblock Copolymer

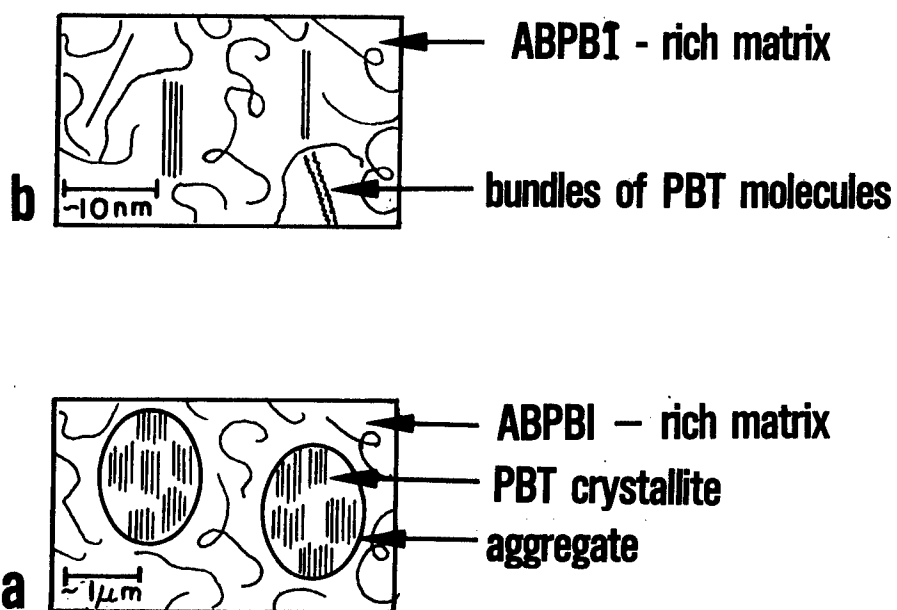


Figure 2. Models for Morphology of a 30% PBT/70% ABPBI Physical Blend
 a) Vacuum Cast Film from $C > C_{cr}$ Solution and b) Spun Fiber
 from $C < C_{cr}$ Solution

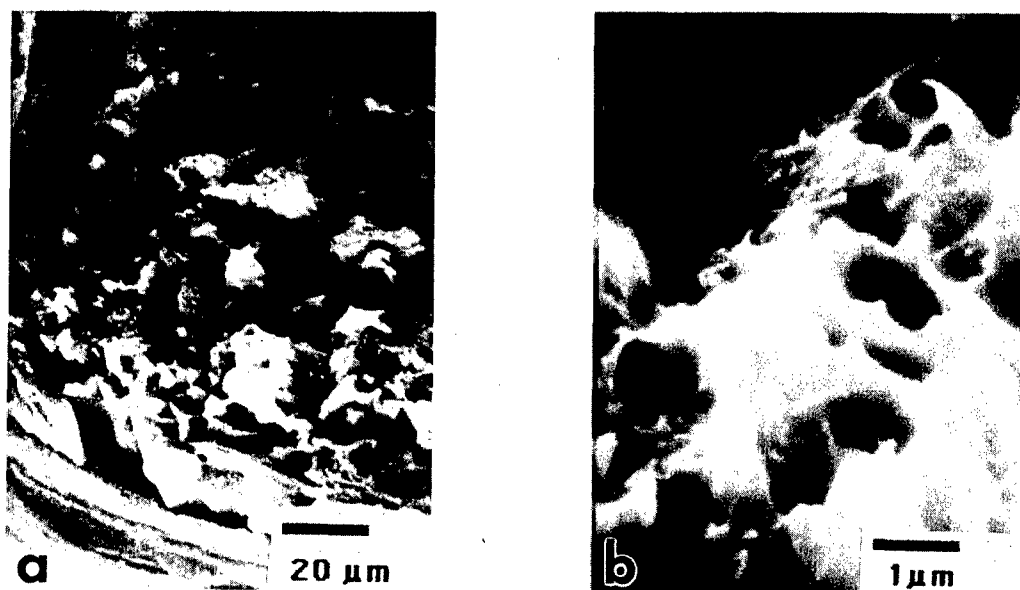


Figure 3. SEM Images of 30% PBT/70% ABPBI Vacuum Cast Copolymer Film at a) Lower Magnification and b) at Higher Magnification

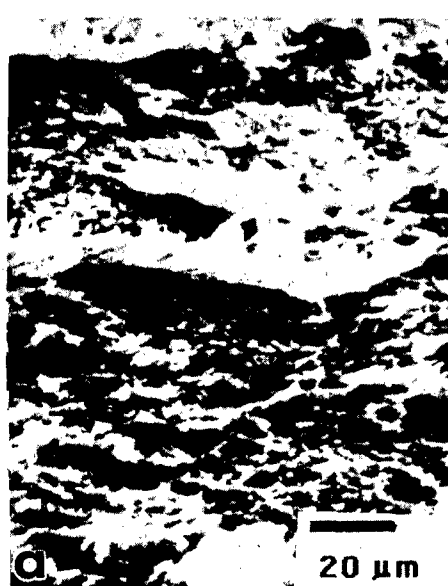


Figure 4. SEM Images of 30% PBT/70% ABPBI Spun Copolymer Fiber at a) Lower Magnification and b) at Higher Magnification

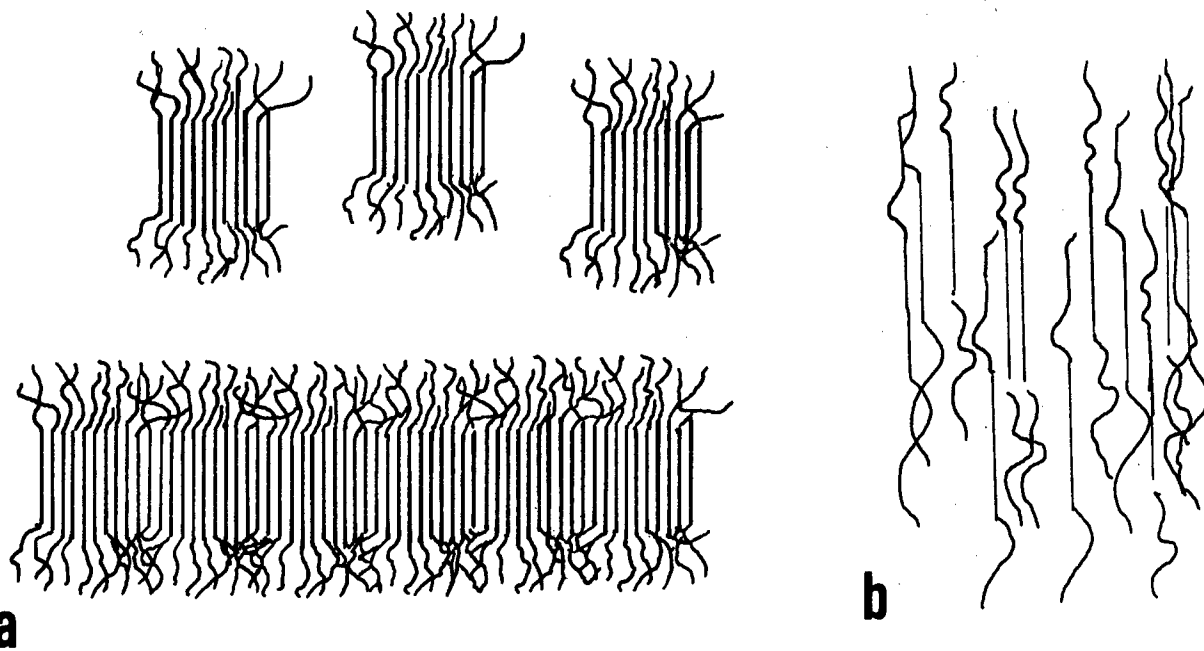


Figure 5. Models for Morphology of a 30% PBT/70% ABPBI Copolymer
a) Vacuum Cast Film from $C > C_{cr}$ Solution and b) Spun Fiber
from $C < C_{cr}$ Solution

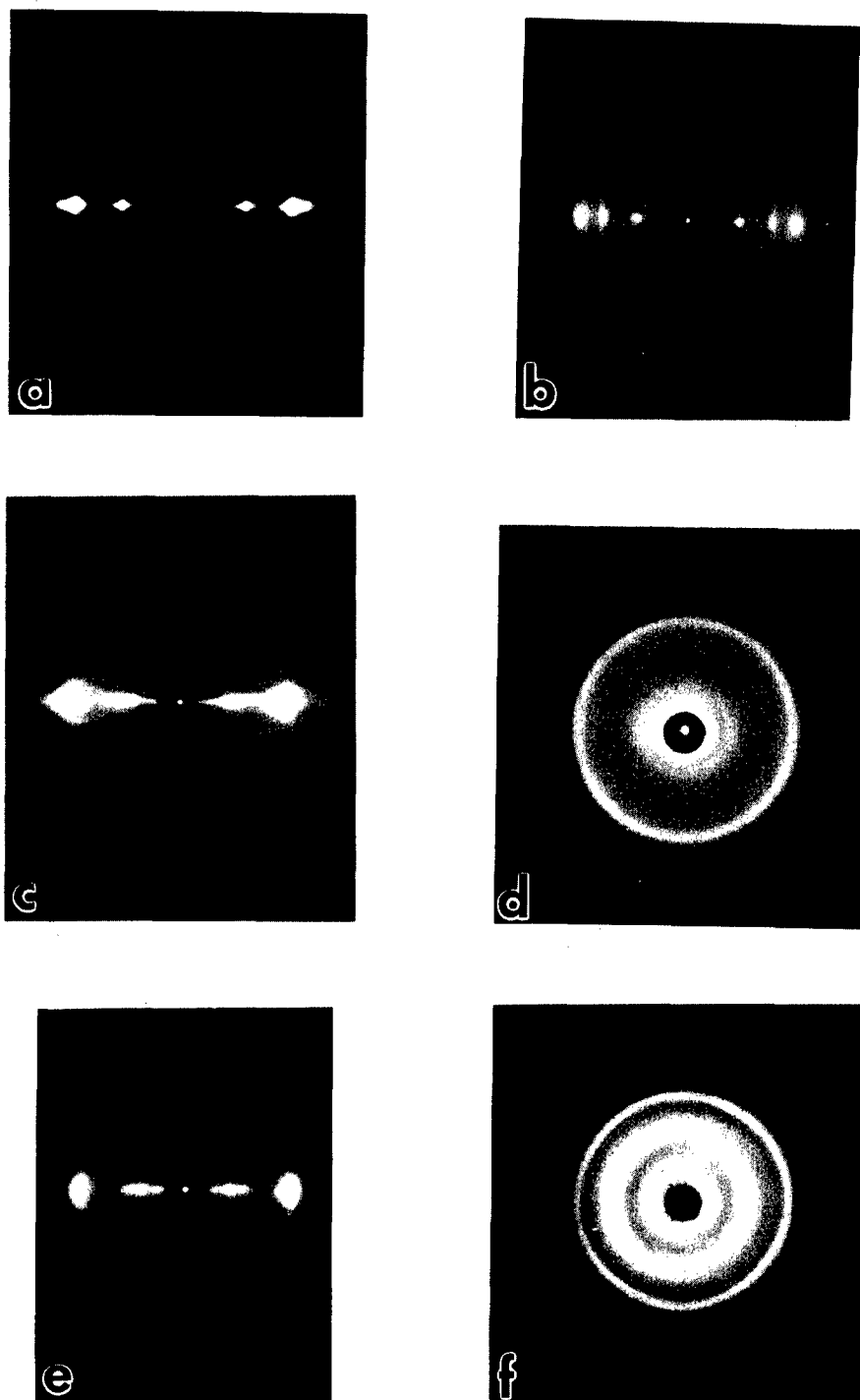


Figure 6. WAXS Laue Photographs of a) PBT Fiber, b) ABPBI Fiber, c) 30% PBT/70% ABPBI Physical Blend Vacuum Cast Film, d) 30% PBT/70% ABPBI Physical Blend Spun Fiber, e) 30% PBT/70% ABPBI Copolymer Vacuum Cast Film, f) 30% PBT/70% ABPBI Copolymer Spun Fiber

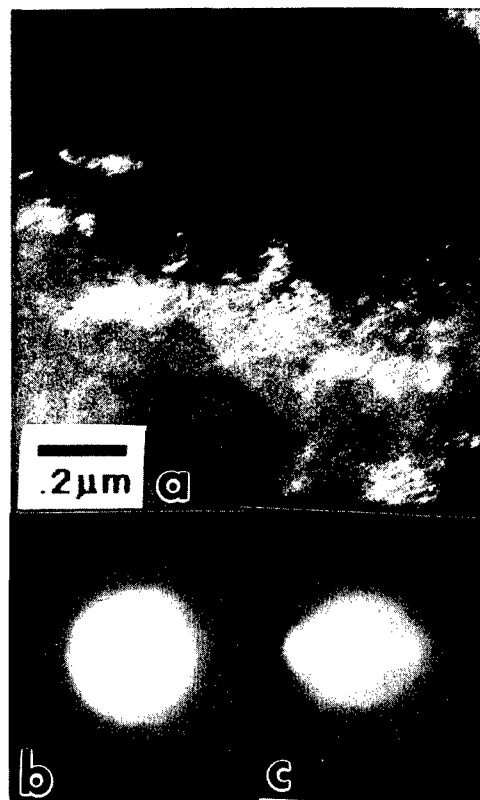


Figure 7. TEM of 30% PBT/70% ABPBI Vacuum Cast Copolymer Film showing a) Dark Field Image, b) SAED Pattern from 5 μm Area, and c) SAED Pattern from 0.1 μm Area

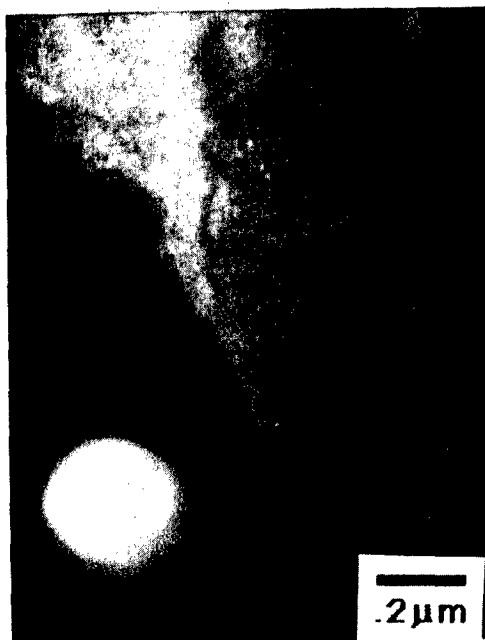


Figure 8.

TEM of 30% PBT/70% ABPBI Spun Copolymer Fiber
showing a) Dark Field Image and b) SAED Pattern